A New Luminous Blue Variable in the Outskirts of the Andromeda Galaxy

Y. Huang[1,11] , H.-W. Zhang[2,3,11], C. Wang[2,10], B.-Q. Chen[1], Y.-W. Zhang[4,5], J.-C. Guo[2,6], H.-B. Yuan[7], M.-S. Xiang[8], Z.-J. Tian[9], G.-X. Li[1], and X.-W. Liu[1]

[1] South-Western Institute for Astronomy Research (SWIFAR), Yunnan University (YNU), Kunming 650500, People's Republic of China; yanghuang@ynu.edu.cn, x.liu@ynu.edu.cn

[2] Department of Astronomy, Peking University (PKU), Beijing, 100871, People's Republic of China; zhanghw@pku.edu.cn

[3] Kavli Institute for Astronomy and Astrophysics, Peking University, Beijing, 100871, People's Republic of China

[4] University of Chinese Academy of Sciences, Beijing 100049, People's Republic of China

[5] Yunnan Observatories, Chinese Academy of Sciences, Kunming 650011, People's Republic of China

[6] Department of Physics and Astronomy, University College London, London WC1E 6BT, UK

[7] Department of Astronomy, Beijing Normal University, Beijing, 100875, People's Republic of China

[8] Max-Planck Institute for Astronomy, Königstuhl, D-69117, Heidelberg, Germany

[9] Department of Astronomy, Yunnan University (YNU), Kunming 650500, People's Republic of China

Abstract

The hot massive luminous blue variables (LBVs) represent an important evolutionary phase of massive stars. Here, we report the discovery of a new LBV—LAMOST J0037+4016 in the distant outskirt of the Andromeda galaxy. It is located in the southwestern corner (a possible faint spiral arm) of M31 with an unexpectedly large projection distance of ∼22 kpc from the center. The optical light curve shows a 1.2 mag variation in V band and its outburst and quiescence phases both last over several years. The observed spectra indicate an A-type supergiant at an epoch close to the outburst phase and a hot B-type supergiant with weak [Fe II] emission lines at an epoch of much dimmer brightness. The near-infrared color–color diagram further shows that it follows the distribution of Galactic and M31 LBVs rather than B[e] supergiants. All the existing data strongly show that LAMOST J0037+4016 is an LBV. By spectral energy distribution fitting, we find it has a luminosity $(4.42 \pm 1.64) \times 10^5 L_\odot$ and an initial mass $\sim 30 M_\odot$, indicating its nature of a less luminosity class of LBV.

Unified Astronomy Thesaurus concepts: Andromeda Galaxy (39); A supergiant stars (8); Luminous blue variable stars (944)

1. Introduction

Luminous blue variables (LBVs) are hot, unstable, massive ($\geqslant 25$–$30 M_\odot$) and extremely luminous (10^5–$10^7 L_\odot$) evolved stars in the upper left parts of the Hertzsprung–Russell (HR) diagram (Conti et al. 1984; Humphreys & Davidson 1994; hereafter HD94). During the LBV phase, massive stars undergo episodes of eruptive mass loss (10^{-5}–$10^{-4} M_\odot$ yr^{-1}), accompanied by spectacular photometric and spectral variabilities, on timescales of years to decades or longer (HD94; van Genderen 2001). The origin of this eruption is not yet well understood, partly due to the limited number of confirmed LBVs and the infrequency of the eruption stage. From the quiescence to the outburst (or eruptive) stage, the brightness of an LBV increases by 1–2 mag in the visual band and the spectrum changes from an O/early B-type supergiant to an A/F-type one.

LBVs are of vital importance for studying the very late stage of massive star evolution. However, the current understanding of the evolutionary status of LBVs is quite uncertain. At present, the LBV is either considered to be a transition phase between the main sequence of massive stars and Wolf–Rayet (WR) stars (e.g., HD94; Maeder & Meynet 2000) or is an intermediate precursor of a supernova (e.g., Smith et al. 2007, 2008, 2011; Trundle et al. 2008; Gal-Yam & Leonard 2009; Groh et al. 2013; Mauerhan et al. 2013; see more details in the review paper by Smith 2014). More recently, Smith & Tombleson (2015) proposed that LBVs

might be evolved blue stragglers, products of binary evolution, although this is still under hot debate (e.g., Davidson et al. 2016; Humphreys et al. 2016; Aadland et al. 2018). Discovery of new LBVs is therefore of vital importance for understanding the origin of the eruption and the role LBVs play in the stellar evolution.

In this Letter, we report the discovery of a new LBV—LAMOST J0037+4016 (R.A.: 00:37:20.65, decl.: +40:16:37.70) in the Andromeda galaxy (M31). The object was originally selected as an M31 blue supergiant candidate for LAMOST (Cui et al. 2012) observation based on its Johnson Q-index (e.g., Massey 1998) calculated using the photometry from the Local Group Galaxy Survey (LGGS; Massey et al. 2006). The resultant radial velocity agrees very well with what was expected as predicted by the rotation curve (Drout et al. 2009) of M31, and thus confirms it is indeed one of the supergiants in M31. This supergiant is in the southwestern corner of M31 at an unexpectedly large projection distance of ∼22 kpc from the center of M31 (see Figure 1). This corner seems to belong to an extended (sub)structure (possibly a faint spiral arm) of the M31 disk, as revealed by the *Herschel* SPIRE 250 μm (Fritz et al. 2012) and 21 cm (Braun et al. 2009) images shown in Figure 1. In Section 2, we describe the photometric and spectroscopic data that we employ in the current work. The main results are presented and discussed in Section 3. In Section 4, the physical properties (e.g., effective temperature, and luminosity) and environments of LAMOST J0037+4016 are derived and discussed, respectively. Finally, we summarize in Section 5.

---

[10] LAMOST Fellow.
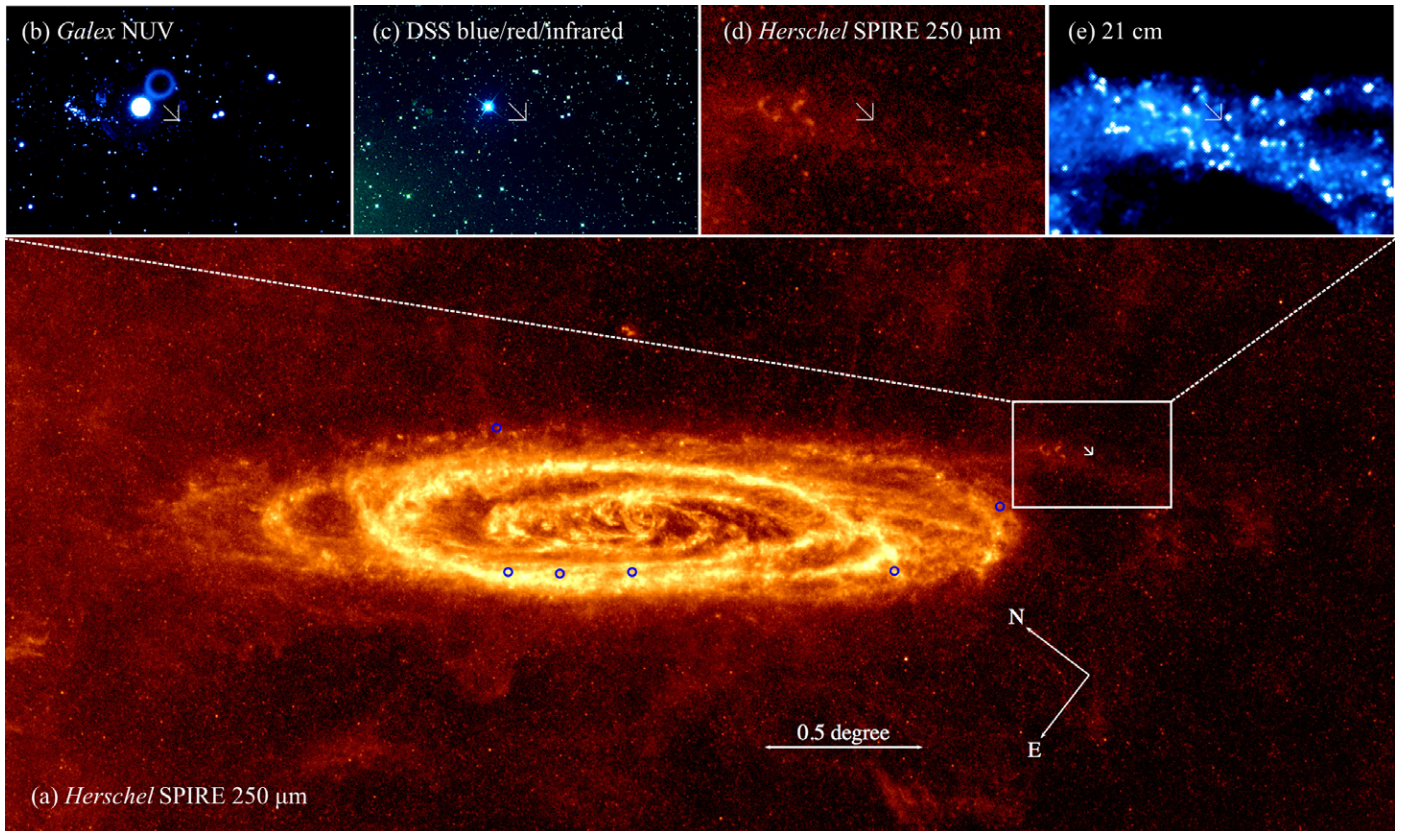[11] Corresponding author.

Figure 1. Images in the different bands to show the location and environment of LAMOST J0037+4016. Panel (a): *Herschel* SPIRE 250 μm image. Spatial scale is shown in the middle-bottom. The six blue circles mark the locations of the confirmed LBVs (Richardson & Mehner 2018) in M31. The white box with sizes of 20′ × 30′ is centered at the location of this newly discovered LBV. The four images on the top zoom in on the area (of the same size of the white box) of LAMOST J0037+4016 in *Galex* NUV band (panel (b)); in DSS blue, red, and infrared color composite image (panel (c)); in the *Herschel* SPIRE 250 μm image (panel (d)) and in the 21 cm image (panel e).

2. Data

To unravel the nature of LAMOST J0037+4016, we first describe the available photometric and spectroscopic data, including both archival and those newly obtained in the current work.

2.1. Photometric Data

The photometric data of LAMOST J0037+4016 employed here are mainly from the Catalina Real Time Transient Survey (CRTS; Drake et al. 2009) and the All-Sky Automated Survey for Supernovae (ASAS-SN; Jayasinghe et al. 2019). From CRTS, measurements of a total of 207 epochs in *V* band are found for LAMOST J0037+4016 over a period of ∼8 yr from 2005 to 2013. All these measurements were collected with the 0.7 m Catalina Schmidt Survey (CSS) telescope located north of Tucson, Arizona. From ASAS-SN, a total of 741 measurements in Johnson *V* band at different epochs are found for LAMOST J0037+4016 over a period of ∼7 yr from 2012 to 2018. We note that only 294 of the 741 measurements with magnitude errors smaller than 0.15 mag are finally adopted in the current analysis.

In addition to the CRTS and ASAS-SN data, we have also included some observations from large-scale multiband optical/near-infrared photometric surveys, including LGGS (*UBVRI*; Massey et al. 2006), SDSS (*ugriz*; Alam et al. 2015), XSTP-GAC (*gri*; Liu et al. 2014; Zhang et al. 2014), and 2MASS (*JHK*$_s$; Skrutskie et al. 2006).

Table 1
Photometric Data Used for LAMOST J0037+4016

UT Date	Facility	Filters	Number of Epochs
1998 Nov 23	2MASS	*JHK*$_s$	1
2000 Oct 4	LGGS	*UBVR*	1
2002 Sep 5	SDSS	*ugriz*	1
2005–2013	CRTS-CSS	*V*	207
2010 Oct 1	XSTP-GAC	*gri*	1
2012–2018	ASAS-SN	*V*	294
2016 Nov 7	NAOC 2.16 m	*BV*	1
2017 Jan 13	YNAO 2.4 m	*UBVRI*	1

Finally, we observed LAMOST J0037+4016 with the 2.16 m telescope of NAOC in Xinglong (XL), China, in *B* and *V* bands on 2016 November 7 and with the 2.4 m telescope of YNAO in Lijiang (LJ), China, in *UBVRI* bands on 2017 January 13. The data were reduced in the standard way with IDL programming language. The resultant magnitudes were then calibrated to the Johnson–Cousins photometric systems. All the photometric observations described above are summarized in Table 1.

2.2. Spectroscopic Data

As mentioned, LAMOST J0037+4016 was selected and targeted by the LAMOST Spectroscopic Survey (Deng et al. 2012; Liu et al. 2014) as a supergiant candidate in M31. It was observed twice by LAMOST, on 2011 October 4 and 29.

Table 2
Spectroscopic Data Used for LAMOST J0037+4016

UT Date	Facility	Wavelength Range (Å)	FWHM (Å)	Exp. Time (s)	Seeing (arcsec)
2011 Oct 4	LAMOST	3700–9000	2.5	1800 × 3	3.2
2011 Oct 29	LAMOST	3700–9000	2.5	900 × 3	2.8
2016 Jan 26	YNAO 2.4 m/YFOSC-G14	3700–7200	11.4	1800	1.3
2018 Jan 22	Palomar 5.1 m/DBSP-B1200	3890–5400	1.4	1200 × 3	1.1
	Palomar 5.1 m/DBSP-R600	5790–9000	2.8		

LAMOST can simultaneously collect up to 4000 optical ($\lambda\lambda$3700–9000), low-resolution ($R \sim 1800$) spectra in one exposure. The data were processed using the LAMOST standard pipeline (Xiang et al. 2015). In addition, LAMOST J0037+4016 was observed on 2016 January 26 and on 2018 January 22 with YFOSC mounted on the 2.4 m telescope of YNAO and with the double spectrograph (DBSP) mounted on 5.1 m Hale telescope. YFOSC is a multimode instrument for imaging and low/medium resolution spectroscopy, working at the Cassegrain focus. A slit width of 1″8 was used with grism 14 (G14), covering 3700–7200 Å at a full width at half maximum (FWHM) resolution of ∼11.4 Å. The DBSP is a low-to-medium resolution (R between 1000 and 10,000) grating instrument and it can obtain spectra in blue and red channels (using a beam splitter), simultaneously. Using a slit of 1″, together with B1200 and R600, we have obtained a blue spectrum covering 3890–5400 Å (FWHM ∼ 1.4 Å) and a red spectrum covering 5790–9000 Å (FWHM ∼ 2.8 Å). The data taken from YFOSC and DBSP were reduced with the standard procedure using IRAF. The details of those spectroscopic observations are summarized in Table 2.

3. Results

3.1. Light Curve

To construct the optical light curve of LAMOST J0037+4016, we first convert measurements in other systems to Johnson V band magnitudes. For the SDSS filter system, we obtain Johnson V magnitudes using the transformation equation of Jester et al. (2005),

$$V = g - 0.58 \times (g - r) - 0.01. \quad (1)$$

For the CRTS-CSS, Johnson V band magnitudes are calculated using the transformation equation of Graham et al. (2015),

$$V = V_{CSS} + 0.31 \times (B - V)^2 + 0.04, \quad (2)$$

where color $B - V$ is adopted as the mean value of measurements given by LGGS, SDSS, and XSTP-GAC.[12] The measurements obtained by LGGS, ASAS-SN, NAOC 2.16 m, and YNAO 2.4 m are already of the Johnson system.

The resultant V band light curve of LAMOST J0037+4016 over a period of ⩾18 yr is presented in Figure 2(a). The plot shows that LAMOST J0037+4016 continued to rise in brightness since the beginning of the data, 2000 October ($V = 15.85$ mag), and reached maximum light (the outburst phase) around 2005 September ($V \sim 15.2$–15.4 mag). The outburst phase lasted about five years. It started to decline from 2011 January and reached minimum light (the quiescence phase) around 2015 January ($V \sim 16.25$–16.50 mag). Until the last

observation at the end of 2018 November, LAMOST J0037+4016 was still at the quiescence phase. Here we note that the large variations within few to tens of days from ASAS-SN photometry are largely contributed from their measurement errors. The current light curve shows a V band amplitude (ΔV) over 1.2 mag and an outburst/quiescence phase lasting several years. Both behaviors suggest that LAMOST J0037+4016 is a typical LBV (HD94).

3.2. Spectra

In addition to the light curve, we have obtained four spectra at different phases of LAMOST J0037+4016. As shown in Figure 2(b1), the top two spectra were taken by LAMOST at the time (2011 October 4 and 29) close to the outburst phase of LAMOST J0037+4016. The two spectra are almost identical, given the small time interval of less than a month. A consistent radial velocity of -488.7 km s^{-1} is derived from both spectra and it agrees very well with what is expected (-497.7 km s^{-1}), as predicted by the rotation curve of M31 (Drout et al. 2009), confirming that LAMOST J0037+4016 belongs to M31. We also note the presence of Hα emissions in both spectra. The third spectrum of LAMOST J0037+4016 was obtained on 2016 January (the quiescence phase) using YFOSC+G14 mounted on Yunnan Observatories (YNAO) 2.4 m with a 1″8 wide slit. The spectral resolution is quite low, $R \sim 500$. The spectrum is plotted in Figure 2(b1) and shows significant variations in Balmer lines (i.e., Hα, Hβ, Hγ, and Hδ) compared to the earlier two LAMOST spectra. Hα became much stronger this time and the other three high-order Balmer lines all turned from absorption to emission. The last spectrum of LAMOST J0037+4016 was obtained on 2018 January (the quiescence phase) using the double spectrograph (DBSP) mounted on the 5.1 m Hale telescope. The spectrum is shown in Figure 2(b1). The emissions of Hβ, Hγ, and Hδ turned to absorptions again. We zoom the blue range of this spectrum in Figure 2(b2) and some weak [Fe II] emission lines are clearly seen.

We further classify the spectral and luminosity type of LAMOST J0037+4016 by comparing the obtained spectra to a collected spectral library using template matching with a least χ-square algorithm. The collected library includes 160 spectra (FWHM ∼ 1.8 Å) of O-type stars from the Galactic O-star catalog (Sota et al. 2011), 40 spectra (FWHM ∼ 2.0 Å) of O/B-type stars from the digital atlas of OB stars (Walborn & Fitzpatrick 1990), and 70 spectra (FWHM ∼ 2.5 Å) of B/A type stars from the MILES spectral library (Sánchez-Blázquez et al. 2006). To provide a uniform spectral library, a smoothing filter was applied to all the collected spectra to achieve a constant FWHM = 2.5 Å for a common spectral range of 4000–4820 Å. When compared to the spectral library, the observed spectra are also degraded to FWHM = 2.5 Å. For the

---

[12] For the latter two surveys, values of color $B - V$ are actually those converted from color $g - r$ (Jester et al. 2005)
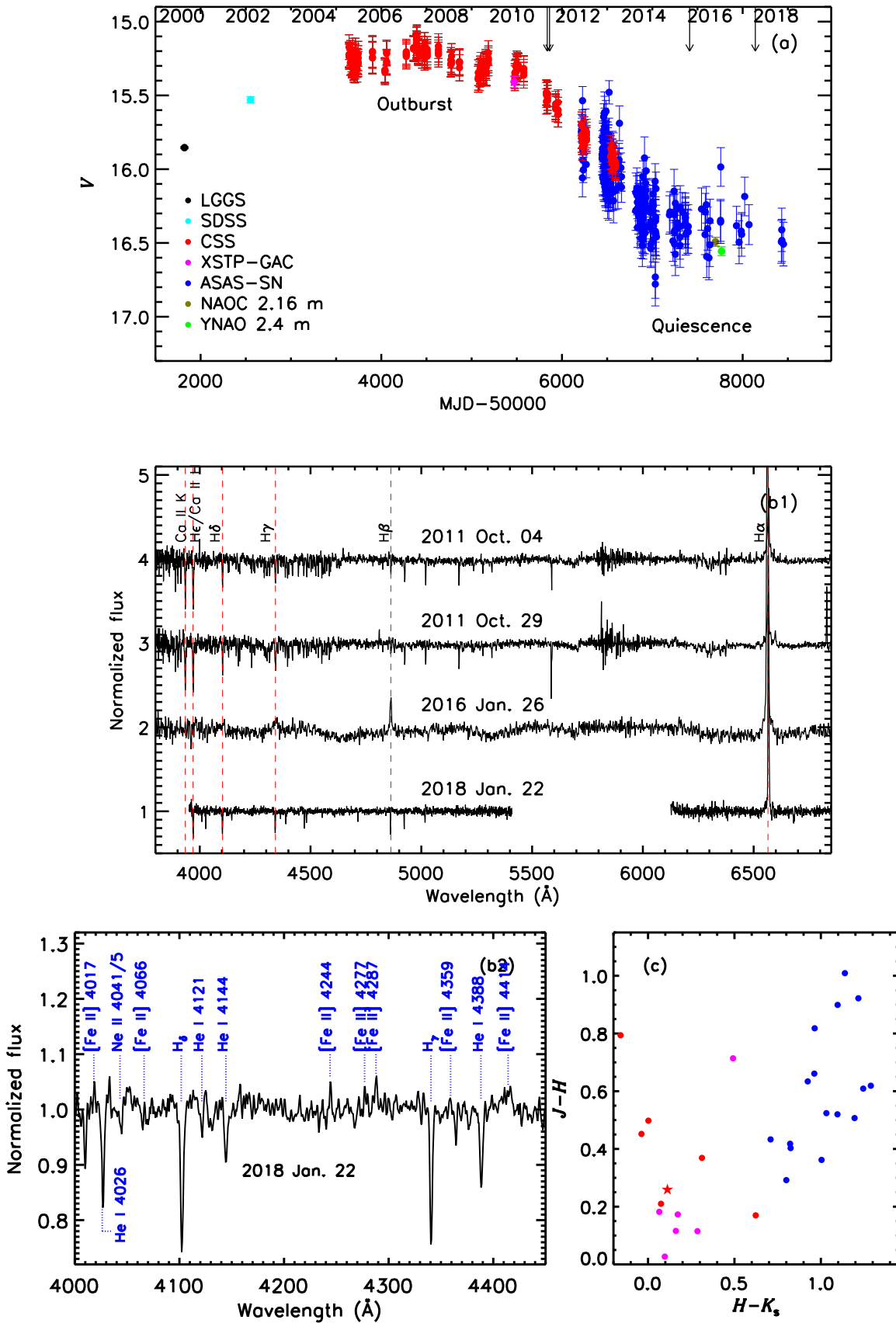
Figure 2. Optical light curve, spectra, and near-infrared color–color diagram of LAMOST J0037+4016. (a) V band light curve of LAMOST J0037+4016 (see Section 3.1). The four arrows mark the dates of the four spectroscopic observations of this target. (b1) Normalized spectra of LAMOST J0037+4016. The Balmer and Ca II lines are identified. (b2) The blue range of the spectrum taken at 2018 January 22. The Balmer, He I, and some weak [Fe II] lines are identified. (c) $J - H$ vs. $H - K_s$ color–color diagram of LBVs and B[e]SGs. Galactic LBVs and B[e]SGs are shown by magenta and blue filled circles, respectively. The six confirmed M31 LBVs are shown by red filled circles. The red filled star represents LAMOST J0037+4016.
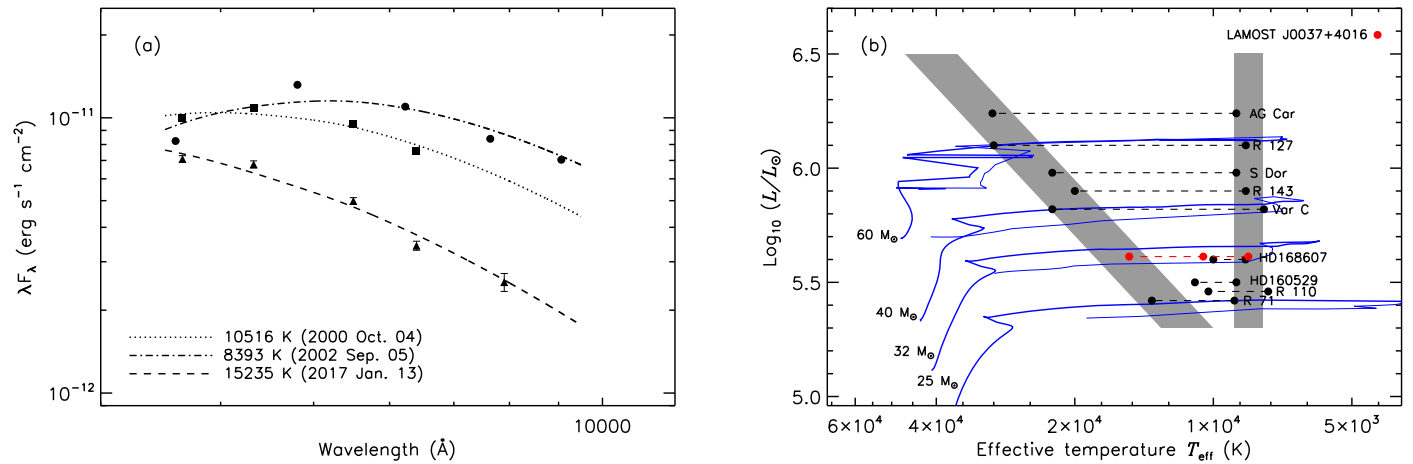
Figure 3. Left panel: SED fitting for LAMOST 0037+4016. Squares, dots, and triangles represent the multiband ($UBVRI/ugriz$) measurements of LGGS, SDSS, and YNAO 2.4 m, respectively. The dashed–dotted, dotted, and dashed lines show the best fits of SEDs based on data from LGGS, SDSS, and YNAO 2.4 m, respectively. The best-fit effective temperatures are labeled at the bottom-left corner of the plot. Right panel: HR diagram of LBVs. The right shaded area represents the outburst phase with a nearly constant effective temperature. The left shaded area represents the diagonal S Doradus instability strip adopted from HD94. Black dots represent well-known LBVs with values of L and $T_{\rm eff}$ adopted from HD94 and de Jager (1998). Red dots represent LAMOST 0037+4016 with values of L and $T_{\rm eff}$ derived in Section 4.1. Also overplotted blue lines are Geneva evolutionary tracks (Ekström et al. 2012) of solar metallicity and an initial rotation speed of 40% of the breakup speed. Here we only include the first 209 points, representing the beginning of any blue loop, for simplicity.

two spectra obtained by LAMOST, they are all classified as A3Ia of an effective temperature around 9000 K, consistent with the expected type/temperature at their observational epochs. We do not obtain the spectral and luminosity type for the third due to its low spectral resolution. For the last spectrum, it is classified as B5/8Ia of an effective temperature around 12,000 K from the template matching. From those spectra, we find that LAMOST J0037+4016 transited from a cool to a warm state from 2011 October to 2018 January, in excellent agreement with the variations seen in the optical light curve.

3.3. Near-infrared Color–Color Diagram

In the upper left parts of an HR diagram, besides the LBVs, there is another type of massive star—B[e] supergiants (B[e] SGs). In some cases, B[e]SGs are found to show variabilities in magnitude and color/spectral-type similar to LBVs (Zickgraf et al. 1996; Clark et al. 2013). To further show LAMOST J0037+4016 is an LBV rather than a B[e] supergiant, we examine it in a near-infrared color–color diagram. As pointed out by Oksala et al. (2013), Kraus et al. (2014), and Humphreys et al. (2017), LBVs and B[e]SGs have distinct infrared colors, given the larger amount of hot dust surrounding a B[e]SG. As Figure 2(c) shows, LBVs and B[e]SGs are indeed well separated in $J - H$ versus $H - K_{\rm s}$ color–color diagram and the LAMOST J0037+4016 follows the distribution of Galactic and M31 known LBVs very well. Therefore, one can conclude that LAMOST J0037+4016 is not a B[e]SG but an LBV.

In summary, all existing data, including the light curve, spectra, and near-infrared colors, suggest that LAMOST J0037 +4016 is an LBV.

4. Physical Properties and Environments of LAMOST J0037+4016

4.1. Physical Properties

In this section, we derive the physical properties of LAMOST J0047+4016 by its spectral energy distribution (SED). Generally, physical parameters estimated in this way could be ambiguous given the well-known degeneracy between the reddening and temperature. However, one can break the degeneracy by the fact that LBVs get cooler (brighter) or hotter (dimmer) with almost constant bolometric luminosity (HD94; Sholukhova et al. 2015).

Assuming $T_{\rm eff}^4 R^2$ and the interstellar reddening (A_V) are both constants, we fit the SED of LAMOST J0037+4016 with the multiband photometric data from LGGS, SDSS, and YNAO 2.4 m, taken at different evolutionary phases of the object. All the data fortunately have measurements in an ultraviolet/blue band. A blackbody is assumed in the SED fitting. The fits are presented in Figure 3. The best-fit yields luminosity and A_V of $(4.42 \pm 1.64) \times 10^5 L_{\odot}$ (assuming a distance to M31 of 752 kpc; Riess et al. 2012) and 0.40 ± 0.05, respectively. The best-fit values of effective temperature and radius are 10516 ± 538 K and $199 \pm 26 R_{\odot}$ on 2000 October 4 (LGGS), 8393 ± 571 K and $308 \pm 56 R_{\odot}$ on 2002 September 5 (SDSS), and 15235 ± 1508 K and $90 \pm 21 R_{\odot}$ on 2017 January 13 (YNAO 2.4 m), respectively. By comparing to the Geneva evolutionary tracks of solar metallicity for an initial rotation velocity of 40% of the breakup speed (Ekström et al. 2012), this LBV is found to have an initial mass around $30 M_{\odot}$. A plot of LAMOST J0037+4016 and some other well-known LBVs (HD94; de Jager 1998) in $T_{\rm eff}$–L HR diagram are also presented in Figure 3. LAMOST J0037+4016 falls in the typical region of LBVs in the diagram, within the standard location of quiescent S Doradus instability strip (HD94) and the constant temperature strip of LBVs at their maximum light phase in S Doradus variations. Finally, as suggested by Humphreys et al. (2016), this new LBV belongs to the less luminous class, that passed through the red supergiant phase and backed again to the left in the HR diagram (HD94).
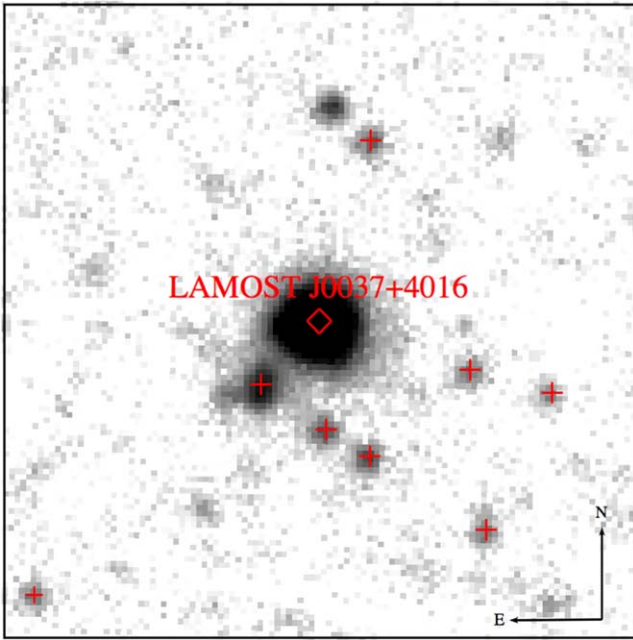
Figure 4. LGGS U band image of LAMOST J0037+4016. The whole field has a size of $30'' \times 30''$, centered at the location of LAMOST J0037+4016 (marked by the red diamond). Here the red crosses mark stars with Q-index smaller than -0.6.

4.2. Environments

As mentioned earlier, LAMOST J0037+4016 is the current most distant LBV in M31, located in the southwestern corner of M31, with an unexpectedly large projection distance of $\sim$22 kpc from the center. As revealed by *Herschel* SPIRE 250 μm (Fritz et al. 2012) and 21 cm (Braun et al. 2009) images, the site of LAMOST J0037+4016 possibly belongs to a faint spiral arm. To show the environments of LAMOST J0037+4016 in detail, the LGGS U band image is shown in Figure 4. In Table 3, we have also listed all the stars with LGGS photometry in UBV bands within $20''$ ($1''$ is about 3.6 pc at the M31 distance) of LAMOST J0037+4016 and most of them (8 out of 10) have Q-index smaller than -0.6 (earlier than a B2 V or a B8 I; Massey 1998). The U band image and the Q-index of the nearby stars of LAMOST J0037+4016 indicate that it may sit within a young massive cluster/star-forming region and it is the most massive one in this cluster/star-forming region. But further spectroscopic observations of those close early-type stars of LAMOST J0037+4016 are required and could further provide vital clues to the recent

debate on the evolutionary status of LBV (e.g., Smith & Tombleson 2015; Davidson et al. 2016; Humphreys et al. 2016).

5. Summary

In this Letter, we report the discovery of a new LBV—LAMOST J0037+4016 in M31, first confirmed as an M31 supergiant in the LAMOST spectroscopic survey. This new LBV is located at the southwestern corner of M31 with an unexpectedly large projection distance of $\sim$22 kpc from the center.

Using archival and newly collected photometric data, we construct a V band light curve of LAMOST J0037+4016 over a time period of 18 yr. The curve reveals a V band variation amplitude of 1.2 mag and both outburst and quiescence phases last over several years. From spectra with the LAMOST, the YNAO 2.4 m telescope and the Hale 5.1 m telescope, we show that LAMOST J0037+4016 displays the characteristics of an A-type supergiant at an epoch close to the outburst phase and a hot early B-type supergiant with weak [Fe II] emission lines at an epoch of much dimmer brightness. From the $J - H$ versus $H - Ks$ color–color diagram, we find that LAMOST J0037+4016 locates in the typical LBV region rather than that of B[e]SGs. We conclude that all existing data strongly suggest that LAMOST J0037+4016 is an LBV.

By SED fitting, we find LAMOST J0037+4016 has a luminosity of $(4.42 \pm 1.64) \times 10^5 L_\odot$ and an initial mass around 30 $M_\odot$, belonging to the less luminosity class of LBV.

Table 3
Stars within $20''$ of LAMOST J0037+4016 with UBV Photometry from the LGGS

Star Name	V (mag)	$B - V$ (mag)	$U - B$ (mag)	Q
J003719.71+401634.3	22.32 ± 0.12	-0.13 ± 0.15	-0.79 ± 0.10	-0.70 ± 0.14
J003719.97+401627.7	22.15 ± 0.08	-0.23 ± 0.10	-0.97 ± 0.07	-0.80 ± 0.10
J003720.04+401635.3	22.00 ± 0.09	0.03 ± 0.10	-1.05 ± 0.05	-1.07 ± 0.09
J003720.44+401646.3	21.85 ± 0.04	-0.24 ± 0.04	-1.07 ± 0.03	-0.89 ± 0.04
J003720.45+401631.5	21.48 ± 0.03	-0.03 ± 0.04	-0.75 ± 0.03	-0.72 ± 0.04
J003720.56+401621.4	19.88 ± 0.01	1.73 ± 0.02	0.85 ± 0.01	-0.39 ± 0.02
J003720.64+401632.7	21.67 ± 0.03	-0.07 ± 0.04	-1.04 ± 0.03	-0.99 ± 0.04
J003720.89+401634.8	20.67 ± 0.02	-0.19 ± 0.03	-0.67 ± 0.02	-0.53 ± 0.03
J003720.89+401635.2	21.11 ± 0.04	-0.06 ± 0.07	-0.88 ± 0.07	-0.84 ± 0.09
J003721.84+401624.9	22.17 ± 0.07	-0.36 ± 0.08	-0.94 ± 0.04	-0.67 ± 0.07

ORCID iDs

Y. Huang ⬤ https://orcid.org/0000-0003-3250-2876

References

Aadland, E., Massey, P., Neugent, K. F., & Drout, M. R. 2018, AJ, 156, 294
Alam, S., Albareti, F. D., Allende Prieto, C., et al. 2015, ApJS, 219, 12
Braun, R., Thilker, D. A., Walterbos, R. A. M., & Corbelli, E. 2009, ApJ, 695, 937
Clark, J. S., Bartlett, E. S., Coe, M. J., et al. 2013, A&A, 560, A10
Conti, P. S., Roussel-Dupre, D., Rensing, M., & Massey, P. 1984, ApJ, 282, 693
Cui, X.-Q., Zhao, Y.-H., Chu, Y.-Q., et al. 2012, RAA, 12, 1197
Davidson, K., Humphreys, R. M., & Weis, K. 2016, arXiv:1608.02007
de Jager, C. 1998, A&ARv, 8, 145
Deng, L.-C., Newberg, H. J., Liu, C., et al. 2012, RAA, 12, 735
Drake, A. J., Djorgovski, S. G., Mahabal, A., et al. 2009, ApJ, 696, 870
Drout, M. R., Massey, P., Meynet, G., Tokarz, S., & Caldwell, N. 2009, ApJ, 703, 441
Ekström, S., Georgy, C., Eggenberger, P., et al. 2012, A&A, 537, 146
Fritz, J., Gentile, G., Smith, M. W. L., et al. 2012, A&A, 546, A34
Gal-Yam, A., & Leonard, D. C. 2009, Natur, 458, 865
Graham, M. J., Djorgovski, S. G., Stern, D., et al. 2015, Natur, 518, 74
Groh, J. H., Meynet, G., & Ekström, S. 2013, A&A, 550, L7
Humphreys, R. M., & Davidson, K. 1994, PASP, 106, 1025
Humphreys, R. M., Davidson, K., Hahn, D., Martin, J. C., & Weis, K. 2017, ApJ, 844, 40
Humphreys, R. M., Weis, K., Davidson, K., & Gordon, M. S. 2016, ApJ, 825, 64
Jayasinghe, T., Stanek, K. Z., Kochanek, C. S., et al. 2019, MNRAS, 486, 1907
Jester, S., Schneider, D. P., Richards, G. T., et al. 2005, AJ, 130, 873
Kraus, M., Cidale, L. S., Arias, M. L., Oksala, M. E., & Borges Fernandes, M. 2014, ApJL, 780, 10
Liu, X.-W., Yuan, H.-B., Huo, Z.-Y., et al. 2014, in Proc. IAU Symp. 298, Setting the Scene for Gaia and LAMOST, ed. S. Feltzing (Cambridge: Cambridge Univ. Press), 310
Maeder, A., & Meynet, G. 2000, ARA&A, 38, 143
Massey, P. 1998, in ASP Conf. Ser. 142, The Stellar Initial Mass Function (38th Herstmonceux Conf.) (San Francisco, CA: ASP), 17
Massey, P., Olsen, K. A. G., Hodge, P. W., et al. 2006, AJ, 131, 2478S
Mauerhan, J. C., Smith, N., Filippenko, A. V., et al. 2013, MNRAS, 430, 1801
Oksala, M. E., Kraus, M., Cidale, L. S., Muratore, M. F., & Borges Fernandes, M. 2013, A&A, 558, 17
Richardson, N. D., & Mehner, A. 2018, RNAAS, 2, 121
Riess, A. G., Fliri, J., & Valls-Gabaud, D. 2012, ApJ, 745, 156
Sánchez-Blázquez, P., Peletier, R. F., Jiménez-Vicente, J., et al. 2006, MNRAS, 371, 703
Sholukhova, O., Bizyaev, D., Fabrika, S., et al. 2015, MNRAS, 447, 2459
Skrutskie, M. F., Cutri, R. M., Stiening, R., et al. 2006, AJ, 131, 1163
Smith, N. 2014, ARA&A, 52, 487
Smith, N. 2016, MNRAS, 461, 3353
Smith, N., Chornock, R., Li, W., et al. 2008, ApJ, 686, 467
Smith, N., Li, W., Foley, R. J., et al. 2007, ApJ, 666, 1116
Smith, N., Li, W., Silverman, J. M., Ganeshalingam, M., & Filippenko, A. V. 2011, MNRAS, 415, 773
Smith, N., & Tombleson, R. 2015, MNRAS, 447, 598
Sota, A., Maíz Apellániz, J., Walborn, N. R., et al. 2011, ApJS, 193, 24
Trundle, C., Kotak, R., Vink, J. S., & Meikle, W. P. S. 2008, A&A, 483, 47
van Genderen, A. M. 2001, A&A, 366, 508
Walborn, N. R., & Fitzpatrick, E. L. 1990, PASP, 102, 379
Xiang, M. S., Liu, X. W., Yuan, H. B., et al. 2015, MNRAS, 448, 822
Zhang, H.-H., Liu, X.-W., Yuan, H.-B., et al. 2014, RAA, 14, 456
Zickgraf, F.-J., Humphreys, R. M., Lamers, H. J. G. L. M., et al. 1996, A&A, 315, 510